

An experimental investigation of discharge/solidification cycle of paraffin in novel shell and tube with longitudinal fins based latent heat storage system

Zakir Khan ^{a*}, Zulfiqar Ahmad Khan ^a

^a Bournemouth University, Faculty of Science and Technology, NanoCorr, Energy and Modelling (NCEM), Fern Barrow, Talbot Campus, Poole, Dorset BH12 5BB, UK.

E-mail: zkhan@bournemouth.ac.uk

Corresponding Author:

^{a*} Bournemouth University, Faculty of Science and Technology, NanoCorr, Energy and Modelling (NCEM), Fern Barrow, Talbot Campus, Poole, Dorset BH12 5BB, UK.

E-mail: zkhan2@bournemouth.ac.uk

Tel.: +44 7459249069

1 Abstract

2 In this article, the discharging cycles of paraffin in novel latent heat storage (LHS) unit are
3 experimentally investigated. The novel LHS unit includes shell and tube with longitudinal fins based
4 heat exchanger and paraffin as thermal energy storage material. The experimental investigations are
5 focused on identifying the transient temperature performance, effective mode of heat transfer,
6 accumulative thermal energy discharge and mean discharge power of paraffin in LHS unit. Moreover,
7 the influences of operating conditions such as inlet temperature and volume flow rate of heat transfer
8 fluid (HTF) on thermal behaviour of LHS unit are experimentally studied. The transient temperature
9 profiles and photographic characterisation of liquid-solid transition of paraffin in LHS unit provide a
10 good understanding of temperature distribution and dominant mode of heat transfer. It is noticed that
11 during discharging cycles, natural convection has an insignificant impact on thermal performance of
12 LHS unit. However, due to inclusion of extended longitudinal fins, conduction is the dominant mode
13 of heat transfer. It is noticed that due to development of solidified paraffin around tubes and
14 longitudinal fins, the overall thermal resistance is increased and thus, discharging rate is affected.
15 However, by regulating inlet temperature or volume flow rate of HTF, the influence of overall thermal
16 resistance is minimised. Mean discharge power is enhanced by 36.05% as the inlet temperature is
17 reduced from 15 °C to 5 °C. Likewise, the mean discharge power is improved by 49.75% as the
18 volume flow rate is increased from 1.5 l/min to 3 l/min. Similarly, with an increase in volume flow
19 rate, the discharge time of equal amount of thermal energy 12.09 MJ is reduced by 24%. It is
20 established that by adjusting operating conditions, the required demand of output temperature and
21 mean discharge power can be attained. Furthermore, this novel LHS unit can meet large scale thermal
22 energy demands by connecting several units in parallel and thus, it has potential to be employed in
23 wide-ranging domestic and commercial applications.

24

25 Keywords

26 Thermal energy storage, Latent heat storage, Discharge cycle, Phase change materials, Heat transfer,
27 Shell and tube heat exchanger

28

29 1. Introduction

30 Due to an increase in global economic growth, the urge for consistent supply of energy has increased
31 in both industrial and domestic applications. Fossil fuels have been serving the purpose of generating
32 desired energy for many decades. However, the harmful emissions from fossil fuels have caused
33 climate change and global warming [1-3]. Therefore, the need for efficient and responsive
34 technologies for renewable energy and heat recovery sources are imperative to abridge gap between
35 energy supply and demand. Thermal energy storage (TES) is an environmental friendly technique to
36 capture thermal energy at solar peak hours or from heat recovery sources and releases it to balance out
37 energy demand. Latent heat storage (LHS) is considered as more attractive technique of TES due to
38 its high thermal storage density, almost isothermal energy storage and retrieval, low vapour pressure,
39 chemical stability and small variation in volume during phase transition [4-6].

40 LHS systems utilises phase change materials (PCM) to capture and release thermal energy during
41 phase transition. LHS systems have been employed in number of practical applications ranging from
42 solar thermal systems, waste heat recovery systems, energy balancing, management and peak shaving,
43 agricultural drying and building air-conditioning systems [7-12]. However, the large scale practical
44 utilisations of LHS systems are hindered by low thermal conductivity of phase change materials (\approx
45 0.2 W/m.K) [13, 14]. Due to low thermal conductivity, the rapid charging and discharging of LHS
46 system is highly affected. Thus, a responsive heat transfer mechanism is essential to counter low
47 thermal conductivity. Several methods have been proposed to improve heat transfer mechanism and
48 consequently overall thermal performance of LHS system such as: container geometrical orientation,
49 inclusion of extended surfaces, dispersion of high conductive additives and encapsulation [15-22].
50 The geometrical configuration of heat exchanger in LHS system plays a crucial role. Various types of
51 heat exchangers for LHS systems are examined, however shell and tube configuration is intensely
52 researched due to its easy installation into majority of industrial applications and design simplicity
53 with minimal heat loss benefits [23].

54 Seddegh et al. [24] performed experimental investigations of paraffin (RT60) in vertical shell and tube
55 configuration with varying tube radius. Four tube radiuses were tested with shell-tube radius ratio of:
56 8.1, 5.4, 4 and 2.7. It was noticed that by decreasing radius ratio from 8.1 to 2.7, the solidification
57 time was reduced by 44%. Yazici et al. [25] performed an experimental examination of paraffin in
58 horizontal shell and tube configuration of LHS system. The effect of eccentricity of heat transfer fluid
59 (HTF) tube on discharging rate was investigated. Six locations were probed with eccentricity values
60 of: -10, -20, -30, 0, 10 and 20. It was noticed that either upward or downward increase in eccentricity
61 showed a reduction in discharging rate, whereas the concentric orientation had presented a relatively
62 higher discharging rate. Similarly, Seddegh et al. [26] numerically examined the thermal behaviour of
63 paraffin (RT50) in vertical and horizontal orientation of shell and tube based LHS system. It was
64 noticed that geometrical orientation of shell and tube had minimal effect on solidification rate, due to
65 conduction dominated heat transfer. Likewise, Longeon et al. [27] experimentally tested paraffin
66 (RT35) in a vertical shell and tube configuration. It was noticed that conduction was the dominant
67 mode of heat transfer during discharging cycle. Hosseini et al. [28] conducted discharging cycles on
68 paraffin (RT50) in horizontal shell and tube based LHS system. It was observed that the initial
69 temperature of liquid paraffin had a negligible impact on overall thermal efficiency. Avci and Yazici
70 [29] conducted experimental investigations on discharging cycles of paraffin in a horizontal shell and
71 tube orientation. It was deduced that conduction was the dominated mode of heat transfer. Moreover,
72 it was observed that discharging rate can be enhanced by decreasing inlet temperature of HTF. Wang
73 et al. [30] numerically examined the influence of inlet temperature and flow rate of HTF on
74 solidification time of n-octadecane in horizontal shell and tube based LHS system. It was noticed that

75 temperature gradient between HTF and PCM was increased by reducing inlet temperature of HTF and
76 thus, the solidification time was significantly reduced. Similarly, it was deduced that flow rate of HTF
77 had an insignificant impact on overall thermal energy capacity of LHS system. Agarwal and Sarviya
78 [31] performed an experimental study on paraffin wax in horizontal shell and tube based LHS system.
79 It was noticed that solidification time was reduced by 19.09% as the mass flow rate was increased
80 from 0.0015 to 0.003 kg/sec. Likewise, the cumulative thermal energy gain by HTF was increased by
81 8.7% with an increase in flow rate from 0.0022 to 0.003 kg/sec. Meng and Zhang [32] conducted
82 numerical and experimental study to identify thermal behaviour of paraffin-copper foam composite in
83 rectangular shaped shell and tube configuration of LHS system. It was observed that by increasing
84 temperature gradient between PCM and HTF, the solidification time can be reduced by 34.76%.
85 Likewise, by increasing inlet velocity of HTF from 0.1 m/sec to 0.2 m/sec, a moderate enhancement
86 of 8.4% was observed in discharging rate. Wang et al. [33] performed experimental examination of
87 erythritol as PCM in vertical shell and tube orientation of LHS system. It was noticed that inlet
88 temperature and flow rate of HTF had a significant impact on discharging rate. However, an increase
89 in pressure of HTF demonstrated a trivial impression on discharging rate.

90 It is evident from previous literature that temperature gradient and flow rate of HTF can influence the
91 discharging rate. However, due to low thermal conductivity of PCM, the optimum benefits could not
92 be achieved. Therefore, the most convenient and cost effective technique is to incorporate extended
93 surfaces [34]. Rabienataj Darzi et al. [35] conducted numerical simulation of n-eicosane in horizontal
94 shell and tube with longitudinal fins. It was noticed that as compared to without fins orientation, the
95 solidification time was increased by 28% to 85% as the number of fins were increased from 4 to 20,
96 respectively. Li and Wu [36] numerically investigated the thermal behaviour of NaNO_3 as PCM in
97 horizontal shell and tube configuration with and without longitudinal fins. It was deduced that
98 solidification time is reduced by 14% with inclusion of longitudinal fins. Rathod and Banerjee [37]
99 conducted experimental examination of stearic acid in a vertical shell and tube with three longitudinal
100 fins configuration. It was observed that due to inclusion of three longitudinal fins, the solidification
101 time was reduced by 43.6%. Liu and Groulx [38] experimentally studied the influence of straight and
102 angled longitudinal fins on discharging rate of dodecanoic acid in horizontal shell and tube
103 configuration. Four longitudinal fins were attached to tube. It was noticed that due to conduction
104 dominated heat transfer, both orientations presented almost identical discharging performance. Al-
105 Abidi et al. [39] performed numerical simulation to investigate the solidification process of paraffin
106 (RT82) in a horizontal triplex tube heat exchanger based LHS system. The discharge time was
107 reduced by 35% with longitudinal fins as compared to no fins configuration. Also, the influence of
108 longitudinal fins number, length and thickness were examined. It was reported that number of fins and
109 length had a significant influence on solidification rate. However, the impact of fins thickness was
110 moderate. Likewise, Almsater et al. [40] performed numerical and experimental investigation on
111 solidification process of water as PCM and Dynalene HC-50 as HTF in a vertical triplex tube heat
112 exchanger. It was observed that the solidification time was reduced from 3.67 hr to 3 hr and 2.31 hr
113 by increasing mass flow rate from 0.02 kg/s to 0.044 kg/s and 0.074 kg/s, respectively. Kabbara et al.
114 [41] conducted experimental investigation on solidification process of dodecanoic acid in a vertical
115 shell and tube with rectangular fins configuration. It was noticed that the solidification rate and
116 discharge power was slightly improved by increasing flow rate. However, more experimental tests
117 could have conducted to help in drawing better conclusions. Agyenim et al. [42] experimentally
118 investigated the influence of radial and longitudinal fins on thermal performance of Erythritol as PCM
119 in shell and tube configuration. It was noticed that cumulative thermal energy discharge for no fins,
120 radial fins and longitudinal fins were 4977.8 kJ, 7293.1 kJ and 8813.1 kJ, respectively. Similarly,
121 Lohrasbi et al. [43] performed comparative examinations on thermal performance of PCM in vertical

122 shell and tube configurations with no fins, optimised circular fins and longitudinal fins. It was
 123 reported that the phase transition rate for optimised circular fins and longitudinal fins orientations
 124 were 3.55 and 4.28 times higher as compared to no fins orientation, respectively. Likewise, Caron-
 125 Soupart et al. [44] conducted experimental investigations of paraffin (RT35HC) in shell and tube with
 126 three configurations: no fins, radial fins and longitudinal fins. It was reported that longitudinal fins
 127 had generated better temperature gradient and thermal power as compared to no fins and radial fins.
 128 Therefore, it is concluded from previous literature that longitudinal fins have better thermal
 129 performance during solidification process as compared to no fins and radial fins configurations.
 130 Moreover, it is observed that shell and tube with single pass orientations are exclusively studied in
 131 previous literature, as detailed in **Table 1**. Therefore, the literature lacks experimental investigations
 132 of shell and tube with multiple passes and extended surfaces. Also, there is a lack of discussion on
 133 thermal energy discharge and mean discharge power of proposed LHS systems. Therefore, there is a
 134 need to experimentally investigate shell and tube with multiple passes and longitudinal fins based
 135 LHS system which can provide a viable solution for higher thermal storage capacity, discharge rate
 136 and discharge power. This article is focused on experimentally investigating a novel geometrical
 137 orientation of shell and tube with multiple passes and longitudinal fins which is not reported in
 138 previous literature. Furthermore, this article proposes a responsive and compact thermal storage
 139 design solution with higher discharge rate, cumulative heat capacity and discharge power.

Table 1

Summary of various studies conducted to examine thermal behaviour of PCM in shell and tube based LHS systems

Ref No.	Study type	Shell and tube		Extended surfaces		PCM
		Tube passes	Orientation	Type	No. of fins	
[24]	Exp.	Single	Vertical	-	-	Paraffin (RT 60)
[25]	Exp.	Single	Horizontal	-	-	Paraffin P56-58
[26]	Num.	Single	Ver. / Hor.	-	-	Paraffin (RT 50)
[27]	Exp./Num.	Single	Vertical	-	-	Paraffin (RT 35)
[28]	Exp./Num.	Single	Horizontal	-	-	Paraffin (RT 50)
[29]	Exp.	Single	Horizontal	-	-	Paraffin P56-58
[30]	Num.	Single	Horizontal	-	-	n-Octadecane
[31]	Exp.	Single	Horizontal	-	-	Paraffin (41-55)
[32]	Exp./Num.	Double	Vertical	-	-	Paraffin (54-64)
[33]	Exp.	Single	Vertical	-	-	Erythritol
[35]	Num.	Single	Horizontal	Longitudinal	4 - 20	n-Eicosane
[36]	Num.	Single	Horizontal	Longitudinal	6	NaNO ₃
[37]	Exp.	Single	Vertical	Longitudinal	3	Stearic acid
[38]	Exp.	Single	Horizontal	Longitudinal	4	Dodecanoic acid
[39]	Num.	Single	Horizontal	Longitudinal	4 - 8	Paraffin (RT 82)
[40]	Exp./Num.	Single	Vertical	Longitudinal	8	Water
[41]	Exp.	Four	Vertical	Rectangular	58	Dodecanoic acid
[42]	Exp.	Single	Horizontal	Circular Longitudinal	8	Erythritol
Present study	Exp.	21	Vertical	Longitudinal	76	Paraffin (RT44HC)

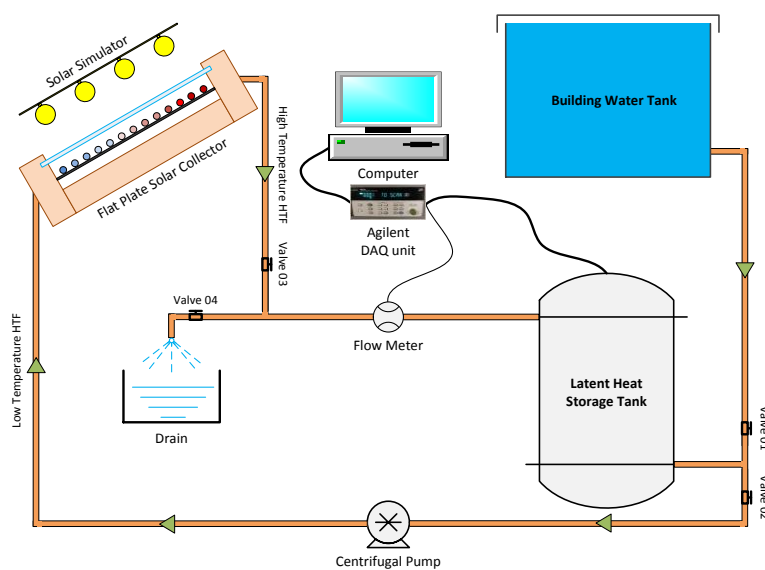
141 In this article, the experimental examinations of discharging cycles of paraffin in a novel LHS system
 142 are conducted. The novel LHS system consists of shell and tube with longitudinal fins based heat
 143 exchanger and paraffin as thermal storage material. The geometrical orientations of novel LHS system
 144 is previously designed, simulated and discussed by authors in [45]. Numerical simulations were
 145 conducted to examine the influence of parameters such as number of tube passes and their orientations
 146 in shell, geometrical configurations of longitudinal fins and construction material; on thermal storage
 147 capacity and charging/discharging rate of LHS system. An optimum design of LHS system was
 148 developed and constructed to perform experimental investigations. Prior to performing discharging
 149 cycles, the paraffin are charged by connecting novel LHS system to flat plate solar collector [46]. In
 150 this article, the discharging cycles are performed by directing cold water from building water tank to
 151 extract thermal energy from paraffin in LHS system. The experimental investigations of discharging
 152 cycles are conducted at various operating conditions of inlet temperature and flow rate of HTF.
 153 Moreover, this paper is focused to examine the transient temperature performance, effective mode of
 154 heat transfer, total solidification/discharge time, cumulative thermal energy discharge and mean
 155 discharge power of paraffin in LHS unit. Furthermore, this article will give comprehensive knowledge
 156 of how to adjust operating conditions or connect several LHS units to meet required thermal energy
 157 demands.

158 2. Experimental Setup and Procedure

159 2.1 Experimental Setup

160 In this article, the focus is on investigation of thermal performance of LHS unit during discharging
 161 process. The schematic representation of experimental setup is demonstrated in **Fig. 1**. The
 162 experimental setup consists of flat plate solar collector (FPSC), solar simulator, latent heat storage
 163 (LHS) unit, paraffin as thermal storage material, water supply from municipal / building, centrifugal
 164 pump, flow meter and data acquisition with computer.

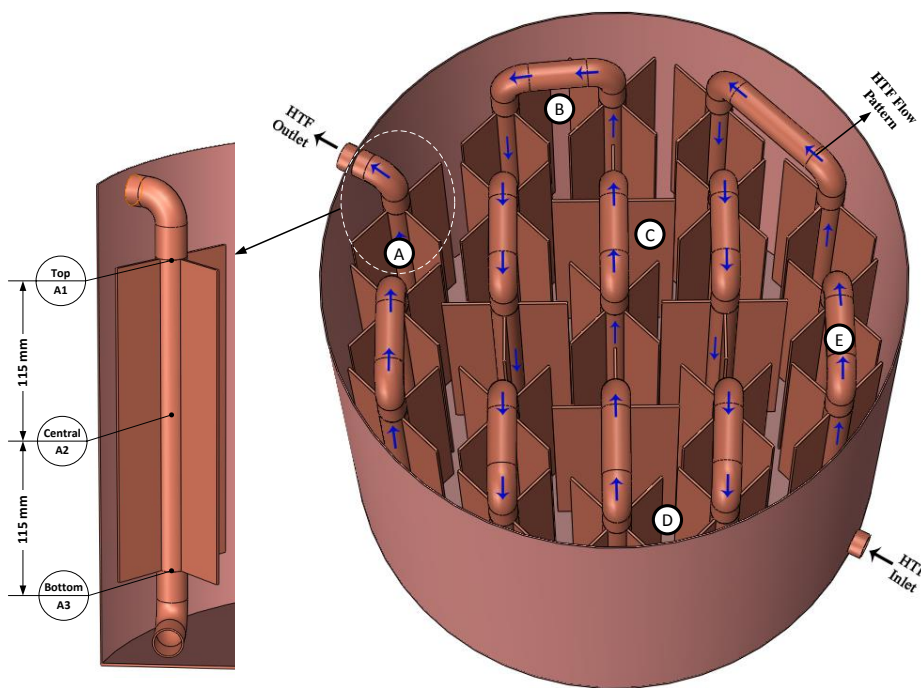
165 FPSC and solar simulators are utilised to conduct charging cycles at various operating conditions.
 166 Solar simulator is operated to deliver steady thermal radiations to FPSC which results in increasing
 167 thermal energy of HTF. The high temperature HTF is guided to pass through LHS unit where it loses
 168 thermal energy to paraffin. Charging cycle is repeated until the temperature of paraffin inside LHS
 169 unit is about 62 °C, which provides a good baseline for all discharging cycles.



170

171 **Fig. 1** Experimental setup layout for conducting discharging cycles of LHS unit.

172 During discharging cycle, the low temperature water is supplied from building water tank to extract
 173 thermal energy from paraffin in LHS unit. LHS unit is composed of vertical shell and tubes heat
 174 exchanger with longitudinal fins and paraffin as thermal storage material. The physical model of LHS
 175 unit is represented in **Fig. 2**. Shell and tubes with longitudinal fins are made up of copper. The outer
 176 diameter, length and thickness of shell are 450 mm, 385 mm and 1 mm, respectively. Likewise, the
 177 outer diameter and thickness of tubes are 22 mm and 1 mm. Longitudinal fins are connected to tubes
 178 having length, width and thickness of 230 mm, 40 mm and 1.5 mm, respectively. Chlorofluorocarbon-
 179 free envirofoam insulator of 50 mm thickness is muffled around the outer surface of shell to minimise
 180 thermal losses. Further design details on LHS unit can be found in [45]. Moreover, paraffin
 181 (RT44HC) is picked as thermal storage material due to its high thermal storage density, long term
 182 thermo-physical stability and good compatibility with copper [14, 47]. Thermal and physical
 183 characteristics of paraffin (RT44HC) are given in **Table 2**. Likewise, water is employed as heat
 184 transfer fluid (HTF).



185

186 **Fig. 2** Physical model representation of LHS unit with longitudinal fins, HTF flow pattern and vertical locations
 187 of thermocouples at various zones.

Table 2

Thermal and physical properties of paraffin (RT44HC) [14, 47]

Phase transition temperature	41-44 °C
Latent heat capacity	255 (kJ/kg)
Specific heat capacity	2.0 (kJ/kg. K)
Thermal conductivity	0.2 (W/m. K) solid, 0.2 (W/m. K) liquid
Density	800 (kg/m ³) solid, 700 (kg/m ³) liquid
Coefficient of thermal expansion	0.00259 (1/K)

188

189 Thermal response of paraffin in LHS unit is recorded by installing 15 K-type thermocouples at five
 190 zones i.e. A, B, C, D and E; at three vertical positions at each zone, as shown in **Fig. 2**. The vertical

191 positions of thermocouples are categorised as top, central and bottom position. Each thermocouple
192 position is at a vertical distance of 115 mm. Moreover, two thermocouples are installed at inlet and
193 outlet of HTF to LHS unit to register the amount of thermal energy discharge by paraffin to HTF.
194 Likewise, a flow meter (Titan FT2 Hall Effect) is utilised to measure volume flow rate value of HTF.
195 The thermocouples and flow meter have an accuracy of $\pm 0.18\%$ and 1.5% , respectively. In
196 discharging cycle, flow control valve 2 and 3 are turned off to bypass FPSC and centrifugal pump,
197 whereas valve 1 and 4 are operated to conduct discharging cycles at various controlled volume flow
198 rates. The data acquisition (Agilent 34972A) is employed to register temperature and volume flow
199 rate readings from thermocouples and flow meter into computer. Time step of 10 s is used to record
200 data on computer.

201 2.2 Experimental Procedure

202 Prior to perform discharging experiments, the paraffin in LHS unit is charged at higher temperature to
203 make sure that entire mass of paraffin is in liquid state. To provide a good baseline, the discharging
204 cycles are started once all thermocouples at top positions at all zones display temperature equal to 62
205 °C.

206 Low temperature water from building water tank is supplied to conduct open loop discharging cycles.
207 To regulate flow rate of water, valve 1 and 4 are adjusted to required value. Discharging cycles are
208 examined at four different volume flow rates of water, such as 1.5, 2.0, 2.5, 3.0 l/min. Low
209 temperature water from building water tank is guided to pass through tube passes in LHS unit. Due to
210 temperature gradient between low temperature water and high temperature paraffin, heat transfer
211 takes place. Paraffin loses thermal energy to water and thus the temperature of water is raised. The
212 high temperature water at outlet of LHS unit can be utilised for desired application. Due to loss of
213 thermal energy to water, paraffin starts solidifying. The discharging cycle is completed once all
214 thermocouples display paraffin temperature less than its phase transition temperature and the
215 temperature difference between inlet and outlet of water is less than 5 °C. Furthermore, to investigate
216 the thermal response of paraffin at various inlet temperatures of water, three different inlet
217 temperatures are tested which are 5, 10 and 15 °C.

218 In order to assess the reliability and repeatability of experimental results, a series of three discharging
219 experiments are conducted at inlet temperature of 10 °C and flow rate of 1.5 l/min. The experimental
220 results illustrate almost identical transient temperature profiles. The statistical standard deviations for
221 discharging rate at top, central and bottom position at zone C are calculated to be 0.008, 0.029 and
222 0.033, respectively.

223 3. Results and Discussion

224 3.1 Temperature Distribution

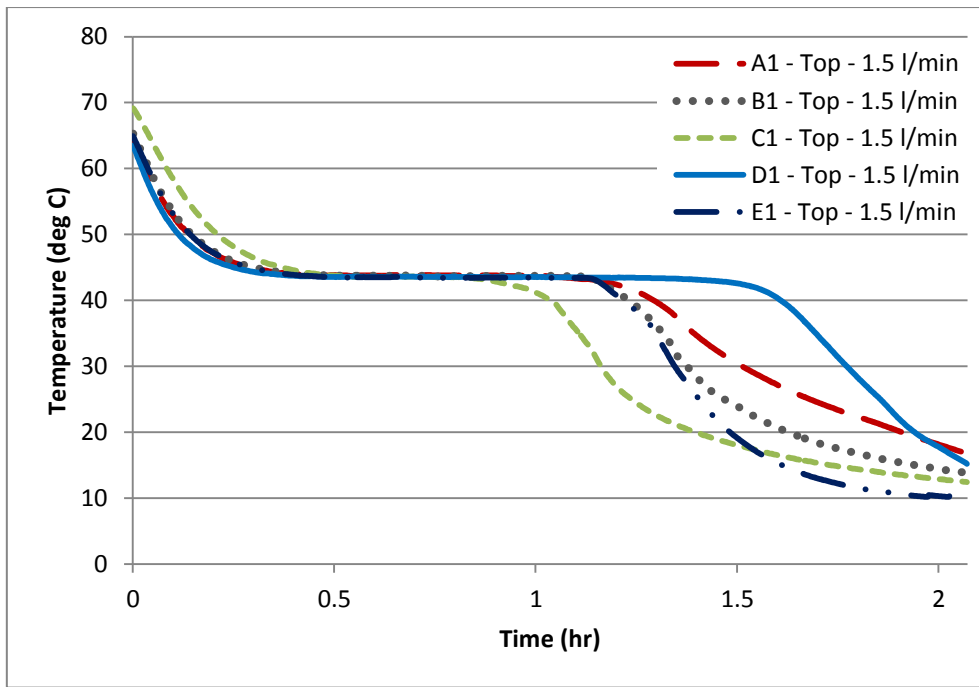
225 To understand the thermal behaviour of paraffin during discharging process, the low temperature HTF
226 at 10 °C is channelled through tubes in LHS unit. Due to temperature gradient, the low temperature
227 HTF extracts thermal energy from high temperature paraffin. In consequence, the temperature of HTF
228 is increased, whereas paraffin temperature is reduced. In order to understand the transient change in
229 thermal energy of paraffin, the temperature data from all fifteen K-type thermocouples are registered.
230 Transient temperature distribution can help in identifying the dominating mode of heat transfer and
231 phase transition rate at various positions in various zones in LHS unit.

232 To perform discharging cycle, a first set of experimental test is conducted with an inlet temperature
233 and flow rate of 10 °C and 1.5 l/min, respectively. The transient temperature profiles acquired from

234 thermocouples at top positions at all five zones are presented in **Fig. 3**. Due to higher temperature
235 gradient between inlet temperature of HTF and paraffin in LHS unit, it is noticed that paraffin at top
236 positions at all five zones rapidly discharges sensible portion of thermal energy to HTF. The sensible
237 portion of thermal energy discharge to HTF is almost linear and as a result, paraffin temperature at top
238 positions is reduced from initial temperature to 44 °C. Subsequently, latent portion of paraffin thermal
239 energy discharge begins. Due to higher latent heat capacity of paraffin, the temperature of paraffin
240 remains almost constant for a good period of time, as shown in **Fig. 3**. During this stage, the
241 temperature of paraffin is gradually reduced from 44 °C to 41 °C. Due to discharge of latent portion of
242 thermal energy, paraffin transforms from liquid phase to mushy phase and subsequently to solid
243 phase. As latent portion of thermal energy is discharged, an instant decline in temperature is observed,
244 which represents the sensible portion of thermal energy discharge.

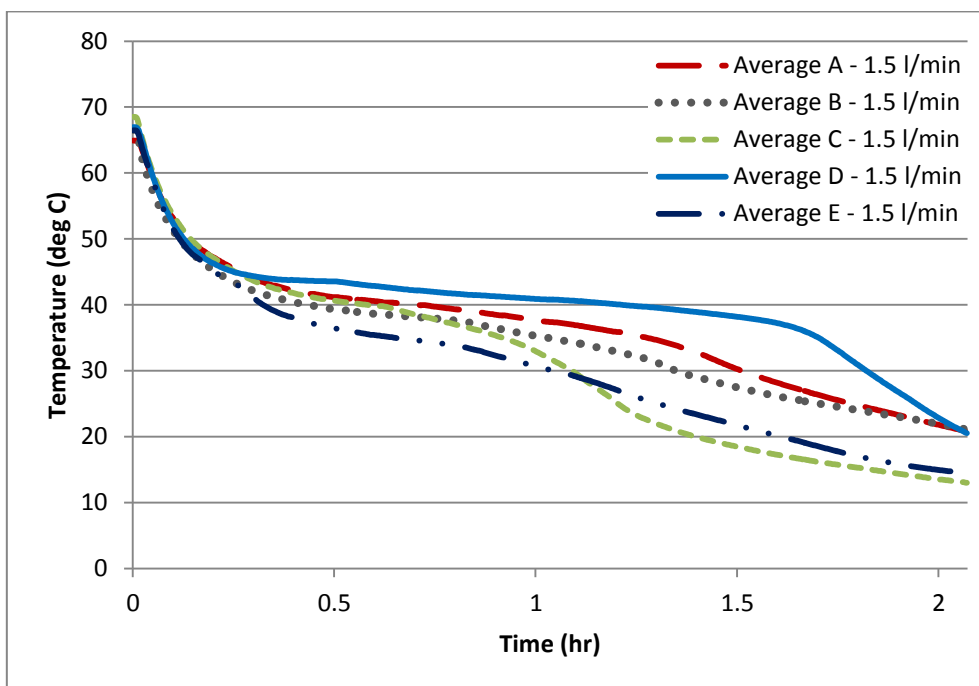
245 Moreover, it can be observed that longitudinal fins are close-packed at zone C (centre of LHS unit), as
246 shown in **Fig. 2**. Hence, the solidification/discharging rate of paraffin at top position at zone C is
247 comparatively higher, as shown in **Fig. 3**. In succession, it can be noticed that due to relatively higher
248 temperature gradient between inlet temperature of HTF and paraffin at zone E, the solidification rate
249 is higher than zone A, B and D. The temperature of HTF increases as it extracts thermal energy from
250 paraffin at zone E, D and C. Therefore, the temperature gradient for heat transfer is slightly reduced as
251 HTF reaches zone B and zone A and thus, it affects the solidification rate of paraffin in those zones.
252 Moreover, it can be observed from **Fig. 2** that HTF tube passes are connected at top at zone B, C and
253 E, whereas it is connected at bottom at zone D. Therefore, due to geometrical orientation of
254 connection between HTF tube passes and insignificant influence of natural convection, the discharge
255 rate is comparatively lower at top position at zone D. Furthermore, an average of temperature profiles
256 is obtained from all three thermocouples (top, central and bottom position) installed at each of five
257 zones, as presented in **Fig. 4**. It is evident that due to higher temperature gradient between inlet
258 temperature of HTF and paraffin, the discharging rate of paraffin at zone E is comparatively higher
259 and is followed by zone C, zone B and zone A.

260 In order to give further insight into thermal performance of paraffin in longitudinal fins based LHS
261 unit, the photographic illustration of discharge cycle is provided in **Fig. 5**. It can be observed that after
262 discharging the system at inlet temperature of 10 °C and volume flow rate of 3 l/min for 0.25 hr, the
263 paraffin around tubes and longitudinal fins are rapidly discharging latent portion of thermal energy to
264 HTF and therefore the formation of solid layer is noticed. The transparent portion of paraffin
265 represents the liquid phase, whereas the white portion displays the solid phase. It can be verified that
266 the paraffin at inlet (zone E) is rapidly transforming to solid as compared to paraffin at outlet (zone
267 A). This is due to the fact that conduction heat transfer and discharging rate is higher at inlet as
268 compared to outlet. Likewise, after discharging for 0.5 hr, it can be noticed that thickness of solidified
269 paraffin around tubes and longitudinal fins is increasing. The increase in thickness at zone E is more
270 prominent. However, the paraffin in between longitudinal fins is still in liquid phase, which
271 demonstrate the low thermal conductivity of paraffin. Similarly, after discharging for 0.75 hr, it is
272 observed that a mushy phase of paraffin is created at top position, whereas the thickness of solidified
273 paraffin has increased around tubes and longitudinal fins. It shows that natural convection has an
274 insignificant impact on solidification of paraffin, whereas conduction is the dominant mode of heat
275 transfer. Further, after discharging for 1 hr, it can be verified that paraffin at top position at zone C is
276 completely solidified, whereas the top positions of the other zones display mushy phase. Finally, after
277 discharging for 1.25 hr, it can be noticed that paraffin at top position at all zones have entirely
278 discharged latent portion of thermal energy and have phase transformed to solid.



279

280 **Fig. 3** Illustration of transient temperature profiles recorded at top position at all five zones during discharging
 281 process. Inlet temperature and volume flow rate of HTF are set to 10 °C and 1.5 l/min.



282

283 **Fig. 4** Time-wise variations in average temperature profiles obtained at all five zones during discharging cycle
 284 at inlet temperature and volume flow rate of 10 °C and 1.5 l/min, respectively.



285

286
287

Fig. 5 Photographic illustrations of solidification front of paraffin in LHS unit during discharging cycle at inlet temperature and volume flow rate of 10 °C and 3 l/min, respectively.

288 3.2 Influence of Inlet Temperature

289 In order to investigate the effect of weather fluctuations on thermal behaviour of paraffin in LHS unit,
290 a series of discharging cycle experiments are conducted at varied inlet temperatures of 5 °C, 10 °C and
291 15 °C. Whereas, the volume flow rate of HTF is set constant to 1.5 l/min. The transient temperature
292 profiles of paraffin acquired from thermocouples installed at top, central and bottom positions within
293 LHS unit are illustrated in **Fig. 6**. Similarly, the time-wise variations in outlet temperatures of HTF
294 are registered, as presented in **Fig. 6**.

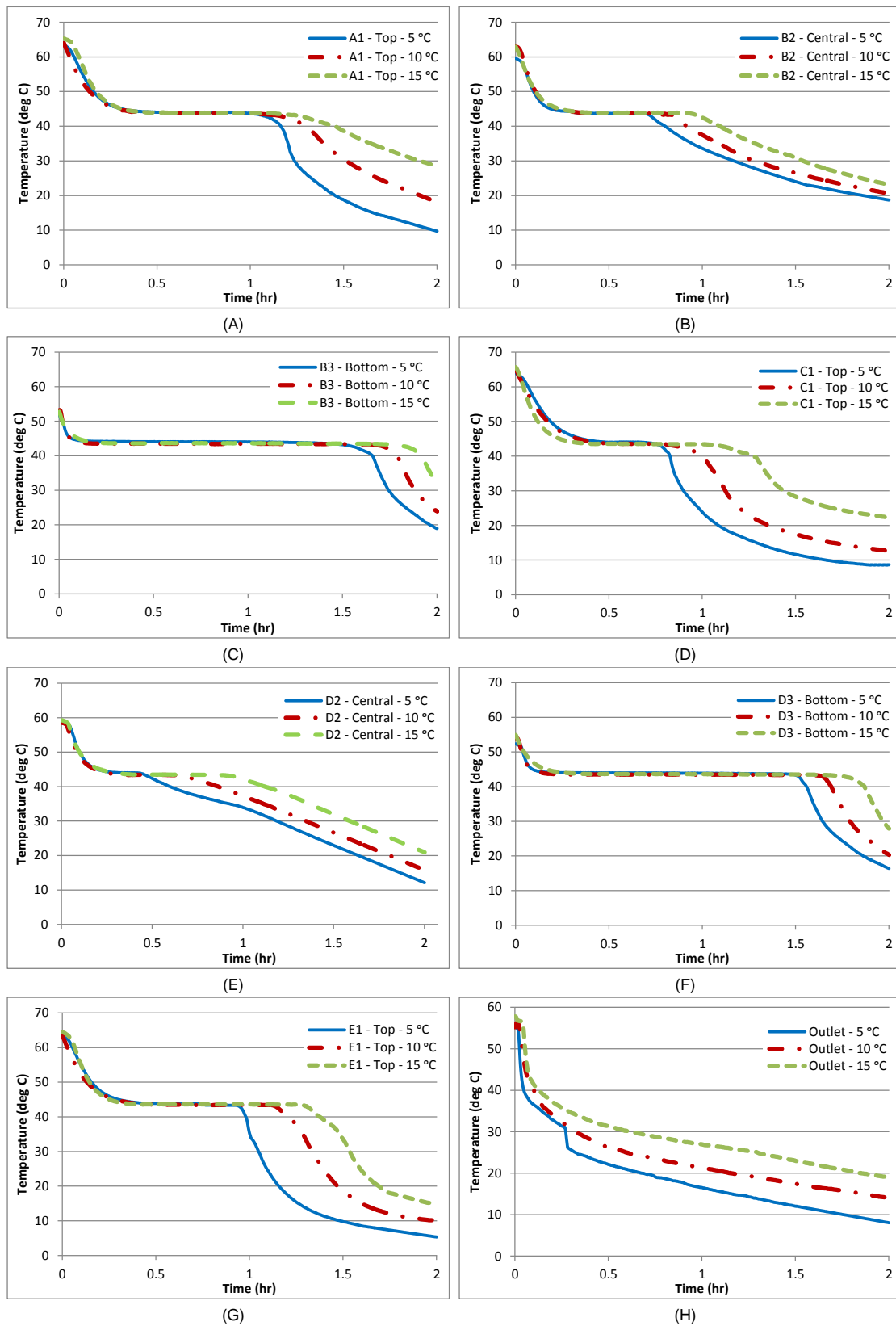
295 It is noticed from experimental investigations that inlet temperature of HTF has a significant impact
296 on discharging rate of paraffin in LHS unit. As shown in **Fig. 6 (A)**, the transient temperature profiles
297 of paraffin at top position at zone A display an identical thermal response to sensible portion of
298 thermal energy discharge at varied inlet temperatures. Therefore, it is noted that inlet temperature of
299 HTF has an insignificant effect on discharging of sensible portion of thermal energy. However, the
300 discharging rate is noticeably influenced during latent portion of thermal energy discharge. The total
301 solidification time for paraffin at inlet temperature of 15 °C is 1.38 hr. However, a higher temperature
302 gradient can be generated by decreasing the inlet temperature of HTF. Therefore, the discharging rate
303 is increased by 9.01 % and 17.43 % as the inlet temperature is decreased from 15 °C to 10 °C and 5
304 °C, respectively. Moreover, it can be observed that after solidification, the sensible portion of thermal
305 energy discharge behave differently to varied inlet temperatures of HTF.

306 The influence of inlet temperature of HTF on transient temperature response of paraffin at central
307 position at zone B and zone D are illustrated in **Fig. 6 (B)** and **Fig. 6 (E)**. It is evident that before
308 solidification, the sensible portion of thermal energy discharge is almost identical for all inlet
309 temperatures of HTF. However, the latent portion of thermal energy is discharged at higher rate by
310 decreasing inlet temperature of HTF. The total solidification time required to discharge the latent
311 portion of thermal energy at central position at zone B is 0.76, 0.88 and 1.06 hr for inlet temperature
312 of 5 °C, 10 °C and 15 °C, respectively. Likewise, the discharging rate at central position at zone D is
313 increased by 23.58% and 48.11% as the inlet temperature is decreased from 15 °C to 10 °C and 5 °C,
314 respectively. After solidification, a linear identical decline in temperature profile is noticed. It shows
315 that conduction is a dominant mode of heat transfer at central position of LHS unit.

316 Likewise, paraffin at top position at zone C indicates a significant enhancement in discharging rate, as
317 shown in **Fig. 6 (D)**. It can be noticed that the discharging rate is increased by 20.36% and 32.95% as
318 the inlet temperature is decreased from 15 °C to 10 °C and 5 °C, respectively. Likewise, paraffin at
319 bottom position at zone D displays a significant reduction in solidification time, as presented in **Fig. 6**
320 **(F)**. The total solidification time is reduced by 9.18% and 16.41% as the inlet temperature is reduced
321 to 10 °C and 5 °C, respectively. Similarly, paraffin at top position at zone E exhibits improvement in
322 discharging rate, as shown in **Fig. 6 (G)**. It can be noticed that an enhancement of 12.37% and 28.04%
323 is recorded by decreasing inlet temperature to 10 °C and 5 °C, respectively. The total solidification
324 time of paraffin at various positions in LHS unit at varied inlet temperatures are presented in **Table 3**.

325 Inlet temperature of HTF has a notable impact on outlet temperature of HTF, as shown in **Fig. 6 (H)**.
326 Due to decrease in inlet temperature of HTF, the temperature gradient between paraffin and HTF is
327 magnified and therefore an enhanced discharge rate is obtained, which results in high temperature
328 output of HTF for a short interval of time. However, with an increase in inlet temperature of HTF, the
329 temperature gradient is reduced and thus a high temperature output is generated for a long period of
330 time. Therefore, it can be predicted that by further increasing the inlet temperature of HTF during

331 discharging cycle, a high temperature output of HTF can be achieved for a longer span of time, which
 332 can be utilised for number of domestic or commercial applications.



333

334 **Fig. 6** Time-wise variation in temperature profile registered at top position (zone A, C and E), central position
 335 (zone B and D), bottom position (zone B and D) and outlet of LHS unit during discharging cycles at various
 336 inlet temperatures (5 °C, 10 °C and 15 °C) and constant volume flow rate of 1.5 l/min.

Table 3

Total solidification time recorded for varied inlet temperatures

Fig. No	Thermocouple		Inlet Temperature		
	Zone	Position	5 °C	10 °C	15 °C
Fig. 6 (A)	A	Top	1.14 hr	1.26 hr	1.38 hr
Fig. 6 (B)	B	Central	0.76 hr	0.88 hr	1.06 hr
Fig. 6 (C)	B	Bottom	1.63 hr	1.76 hr	1.89 hr
Fig. 6 (D)	C	Top	0.81 hr	0.97 hr	1.21 hr
Fig. 6 (E)	D	Central	0.55 hr	0.81 hr	1.06 hr
Fig. 6 (F)	D	Bottom	1.54 hr	1.68 hr	1.84 hr
Fig. 6 (G)	E	Top	0.97 hr	1.18 hr	1.35 hr

337

338 3.3 Influence of Flow Rate

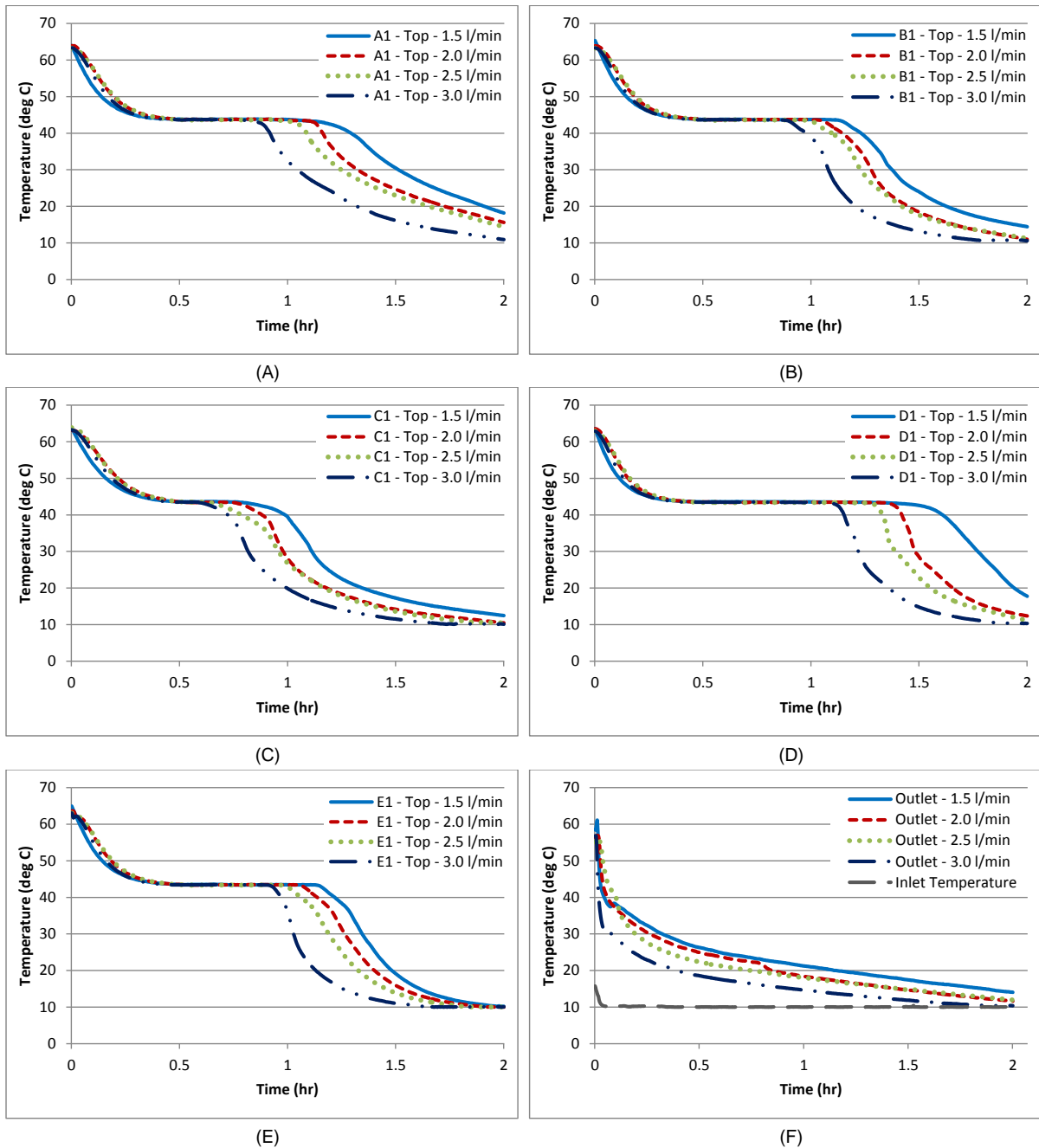
339 To examine the influence of volume flow rate of HTF on heat transfer rate and solidification time of
 340 paraffin in LHS unit, experimental tests are conducted at constant temperature of 10 °C and four
 341 varied volume flow rates of 1.5, 2, 2.5 and 3 l/min. The time-wise variations in temperature profiles
 342 are obtained from thermocouples installed at top position at all five zones and outlet of HTF from
 343 LHS unit, as illustrated in **Fig. 7**.

344 As discussed in **section 3.1**, the discharging cycle of paraffin is composed of three phases. In initial
 345 phase, the sensible portion of thermal energy is discharged rapidly due to higher temperature gradient
 346 between HTF and paraffin. Natural convection is dominating the initial stage of discharging cycle and
 347 thus, the temperature drop of paraffin is fast. In second phase, the latent portion of thermal energy is
 348 discharged at almost isothermal temperature. During this phase, the phase transition from liquid to
 349 solid takes place and thus, the natural convection is weakened and conduction is the dominant mode
 350 of heat transfer. However, due to formation of solidified paraffin around tubes and longitudinal fins,
 351 the overall thermal resistance offered by paraffin is increased which effects the heat transfer rate.
 352 Therefore, it is noticed that latent portion of thermal energy is gradually discharged. In third phase,
 353 the sensible portion of thermal energy in solid phase is discharged which is dominated by conduction
 354 heat transfer. Similarly, it can be noticed from **Fig. 7** that initial sensible phase of thermal energy
 355 discharge is not affected by volume flow rate. However, the latent portion of thermal energy discharge
 356 is noticeably influenced.

357 Paraffin at top position at zone A has demonstrated an obvious enhancement in discharging rate and
 358 reduction in solidification time, as presented in **Fig. 7 (A)**. The total solidification time is reduced by a
 359 fraction of 9.03%, 14.98% and 28.19% as the volume flow rate is increased from 1.5 l/min to 2, 2.5
 360 and 3 l/min, respectively. Likewise, paraffin at top position at zone B has illustrated an increase in
 361 discharge rate by a fraction of 7.16%, 11.55% and 21.01%, as shown in **Fig. 7 (B)**. Similarly, the
 362 solidification time for paraffin at top position at zone C is reduced by 11.04%, 21.22% and 27.32% as
 363 the volume flow rate is increased from 1.5 l/min to 2, 2.5 and 3 l/min, as presented in **Fig. 7 (C)**. Also,
 364 an enhancement in discharging rate is noticed for paraffin at top position at zone D, as illustrated in
 365 **Fig. 7 (D)**. The discharging rate is improved by a fraction of 10.72%, 16.52% and 27.76% as the
 366 volume flow rate is increased. Moreover, the improvement in heat transfer rate is observed for
 367 paraffin at top position at zone E, as shown in **Fig. 7 (E)**. Due to enhanced heat transfer rate, the
 368 solidification time is reduced by 6.76%, 13.05% and 19.81%, respectively.

369 It is evident that in case of constant inlet temperature of HTF, the heat transfer rate can be
 370 significantly influenced by varying volume flow rate of HTF and consequently, the discharging rate of

371 paraffin in LHS unit can be influenced. With an increase in volume flow rate of HTF, the discharging
 372 time is reduced. It is due to the fact that by increasing volume flow rate, the amount of thermal energy
 373 carried away by HTF is also increased. Therefore, the rapid decline in output temperature of HTF is
 374 noticed, as shown in **Fig. 7 (F)**. However, in order to maintain a higher outlet temperature of HTF for
 375 longer period of time, a small volume flow rate is recommended. In practical applications, the volume
 376 flow rate should be regulated to application based demands of outlet temperature and duration of
 377 discharge time.



378

379 **Fig. 7** Transient temperature variations recorded at top position at all five zones and outlet of LHS unit while
 380 conducting discharging cycles at four varied volume flow rates of 1.5, 2.0, 2.5 and 3.0 l/min and constant inlet
 381 temperature of 10 °C.

382 3.4 Energy Discharge and Mean Power

383 In order to investigate the thermal performance of paraffin in longitudinal fins based LHS unit during
384 discharging cycles, the accumulative thermal energy discharge to HTF and mean discharge power of
385 LHS system are calculated. To calculate thermal energy discharge by paraffin to HTF and mean
386 discharge power, the following relations are implemented:

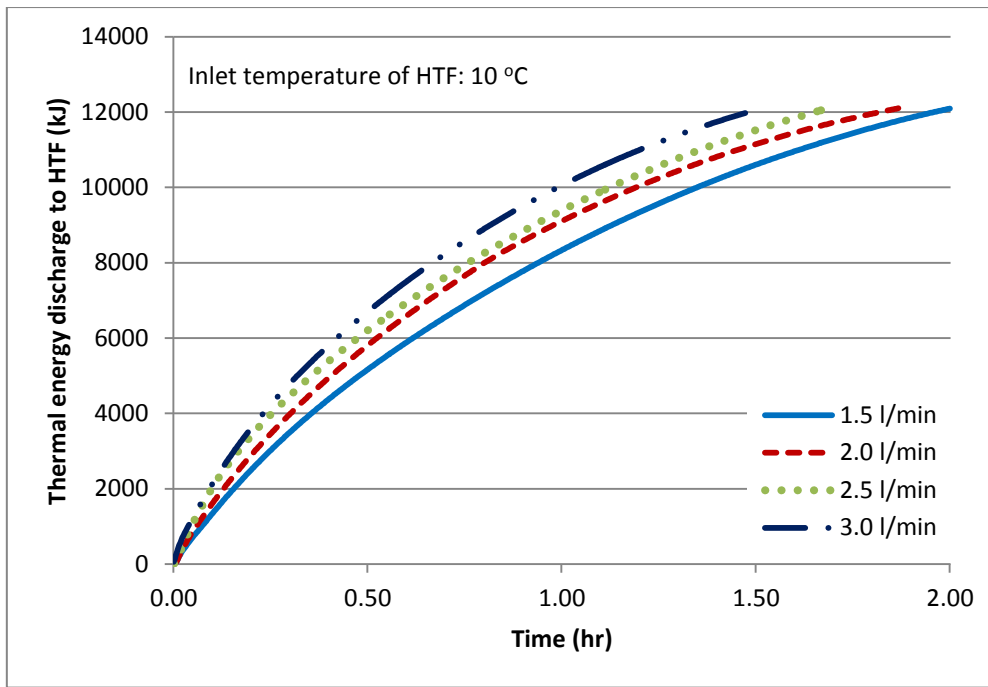
$$387 \quad Q_{dis} = \sum \rho_{avg} \left(\frac{c_{p,in} + c_{p,out}}{2} \right) (T_{HTF,out} - T_{HTF,in}) \dot{V} \Delta t \quad (1)$$

$$388 \quad P_{dis} = \frac{Q_{dis}}{t_{dis}} \quad (2)$$

389 where Q_{dis} , ρ_{avg} , c_p , T_{HTF} , \dot{V} and Δt represent the measure of thermal energy discharge to HTF
390 (kJ), average density of HTF (kg/m^3), specific heat capacity of HTF (kJ/kg. K), temperature of HTF
391 ($^{\circ}\text{C}$), volume flow rate of HTF (m^3/sec) and time interval to record temperature data (sec),
392 respectively. Likewise, P_{dis} represents the mean discharge power of LHS unit (kW) and t_{dis} is the total
393 time elapsed by discharging cycle (sec).

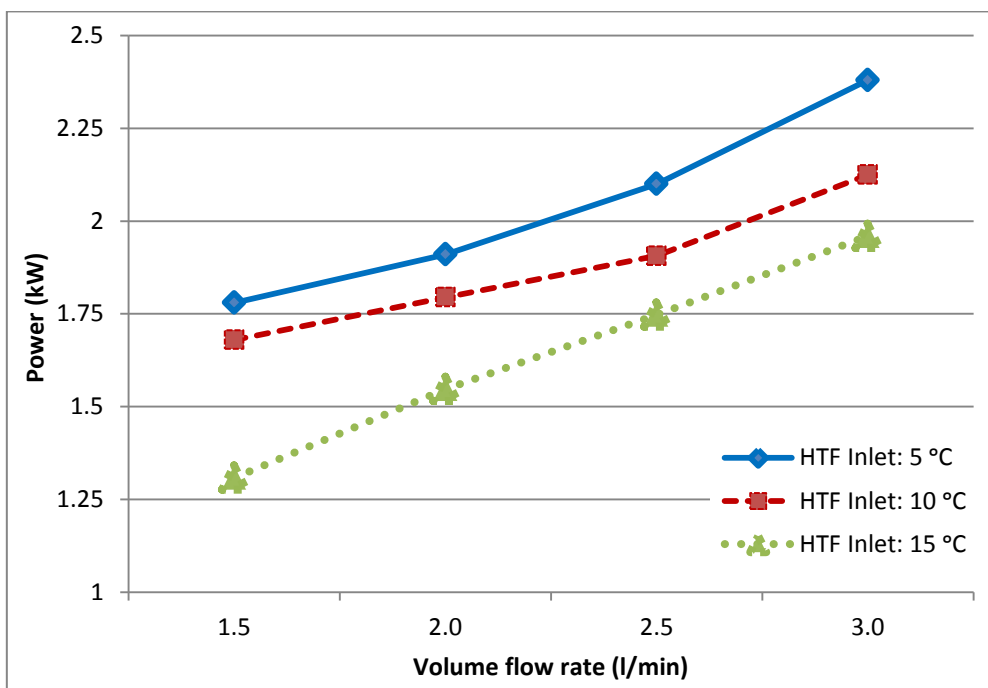
394 Transient variations in thermal energy discharge to HTF is registered by conducting discharge cycles
395 at constant inlet temperature of 10°C and varied volume flow rates of 1.5, 2, 2.5 and 3 l/min, as
396 illustrated in **Fig. 8**. It can be observed that volume flow rate has a significant impact on discharging
397 rate of thermal energy to HTF. Due to higher temperature gradient at start of discharging cycle, the
398 rate of accumulative thermal energy gain by HTF is higher. However, the temperature gradient is
399 reduced owing to extraction of thermal energy from paraffin. Hence, the rate of accumulative thermal
400 energy gain by HTF is affected. Despite that, with an increase in volume flow rate of HTF, the
401 resistance to convective heat transfer in HTF can be decreased and thus, the discharging rate can be
402 enhanced. It is noticed that after 1.5 hr of discharging cycles, the accumulative thermal energy
403 discharge to HTF is recorded as 10604.41 kJ, 11150.88 kJ, 11521.10 kJ and 12055.03 kJ for volume
404 flow rate of 1.5, 2, 2.5 and 3 l/min, respectively. Similarly, in order to discharge equal amount of
405 thermal energy (12094.34 kJ), the required time is reduced by 24% as the volume flow rate is
406 increased from 1.5 to 3 l/min.

407 The impact of inlet temperature and volume flow rate on mean discharge power of LHS unit is
408 illustrated in **Fig. 9**. It can be observed that during inlet temperature of 15°C , the increase in mean
409 power is almost linear with an increase in volume flow rate. The discharge power is enhanced by
410 18.24%, 33.58% and 49.75% by increasing volume flow rate from 1.5 to 2, 2.5 and 3 l/min,
411 respectively. Likewise, for inlet temperature of 10°C , the discharge power is increased by 6.85%,
412 13.47% and 26.49%, respectively. Similarly, for inlet temperature of 5°C , the discharge power is
413 improved by 7.31%, 17.98% and 33.70%, respectively. Moreover, it can be noticed that inlet
414 temperature also significantly influences the mean discharge power. For instance, at constant volume
415 flow rate of 1.5, the discharge power is increased by 28.39% and 36.05% as the inlet temperature is
416 decreased from 15°C to 10°C and 5°C , respectively. Similarly, at flow rate of 3 l/min, the discharge
417 power is increased from 1.959 kW to 2.125 and 2.38 kW, respectively. By regulating inlet
418 temperature and volume flow rate of HTF, the desired output temperature and power demand can be
419 achieved in practical applications.



420

421 **Fig. 8** Transient variation in accumulative thermal energy gain by HTF during discharging cycles at constant
 422 inlet temperature of 10 °C and four different volume flow rates of 1.5, 2.0, 2.5 and 3.0 l/min.



423

424 **Fig. 9** Influence of volume flow rate and inlet temperature of HTF on mean discharging power of LHS unit.

425 Furthermore, the results indicate that the discharge rate, accumulative thermal energy discharge and
 426 mean discharge power of our proposed LHS system is considerably higher as compared to LHS
 427 systems discussed in previous literature, as presented in **Table 4**. It can be noticed that none of the
 428 previously reported models could match the rapid solidification time (1.5 hr), accumulative thermal
 429 energy discharge (12 MJ) and mean discharge power (2.125 kW) of our proposed LHS system.

Table 4
Comparative thermal enhancement achieved by present study

Ref No.	Discharge		
	Time (hr)	Energy (kJ)	Power (kW)
[24]	12.5	575	-
[28]	8.67	772.4	0.025
[30]	0.56	80	-
[31]	18.35	1200	0.02
[32]	0.506	490	0.269
[33]	4.2	-	0.325
[40]	2.31	-	1
[41]	22	7500	0.1
[42]	1.67	7293.1	-
[42]	2.167	8813.1	-
Present study	1.5	12000	2.125

430

431 **4. Conclusions**

432 In this article, the experimental investigations of discharging cycles of paraffin in LHS unit are
 433 presented. LHS unit is comprised of shell and tube with longitudinal fins based heat exchanger and
 434 paraffin as thermal storage material. Water is employed as HTF and is channelled to pass through the
 435 tubes of LHS unit to extract thermal energy from paraffin. The discharging cycles are conducted at
 436 various operating conditions of inlet temperature and flow rate of HTF. The following conclusions are
 437 drawn from experimental investigations of discharging cycles:

- 438 • Due to inclusion of longitudinal fins, the effective surface area for heat transfer is enhanced and
 439 hence the impact of low thermal conductivity of paraffin on discharging cycle of LHS unit is
 440 significantly decreased. Consequently, the discharging rate is significantly improved. The novel
 441 geometrical orientation of shell and tube with longitudinal fins based LHS unit qualifies as an
 442 efficient and responsive thermal energy storage/discharge device. For instance, the novel LHS
 443 unit can discharge 12 MJ of thermal energy to HTF in 1.5 hours when it is discharged at inlet
 444 temperature and volume flow rate of 10 °C and 3 l/min, respectively.
- 445 • It is noticed that natural convection has minimal impact on discharging rate. However, due to
 446 presence of extended surfaces via longitudinal fins, conduction heat transfer is dominant mode
 447 for thermal energy discharge. Moreover, it is noticed that conduction is more prominent at
 448 central position as compared to top and bottom positions of LHS unit. Heat transfer rate is
 449 relatively weaker at bottom position and therefore, the solidification time for paraffin at bottom
 450 position is higher as compared to central and top position.
- 451 • Discharging cycle involves three phases of paraffin. Initially, the sensible portion (liquid phase)
 452 of thermal energy is rapidly discharged due to higher temperature gradient. Secondly, during
 453 latent portion of thermal energy discharge, a rather steady and gradual reduction in temperature

454 is noticed due to high latent heat capacity of paraffin. Likewise, the formation of solidified
455 paraffin around tubes and longitudinal fins increase the overall thermal resistance, which
456 affects the discharging rate. Finally, due to low temperature gradient, the sensible portion (solid
457 phase) of thermal energy discharge is relatively slow as compared sensible portion of liquid
458 phase.

- 459 • It is observed that inlet temperature and volume flow rate of HTF have significant influence on
460 latent portion of thermal energy discharge. The influence of an increase in overall thermal
461 resistance can be controlled by adjusting inlet temperature or volume flow rate of HTF. It is
462 noticed that as the inlet temperature of HTF is decreased from 15 °C to 5 °C, the mean
463 discharge power is enhanced by 36.05%. This is due to the fact that with an increase in
464 temperature gradient, the conduction heat transfer overcomes the overall thermal resistance of
465 paraffin. Likewise, with an increase in volume flow rate from 1.5 l/min to 3 l/min, the
466 solidification time at constant inlet temperature of 10 °C is reduced by 24% to discharge same
467 amount of thermal energy 12.09 MJ. Moreover, in case of constant inlet temperature as 5 °C
468 and 15 °C, the mean discharge power can be enhanced by 33.70% and 49.75% by increasing
469 volume flow rate from 1.5 l/min to 3 l/min, respectively.
- 470 • It is deduced that by adjusting inlet temperature and volume flow rate, the required output
471 temperature and mean power can be achieved in practical applications. Likewise, the novel
472 LHS unit offers time, spatial and economic benefits. Moreover, in order to meet application
473 based energy demands, the mean power and thermal storage capacity can be augmented by
474 connecting several LHS units in parallel. Therefore, the LHS unit can be perfectly employed in
475 various domestic and commercial applications such as heating, ventilation and air conditioning
476 (HVAC) systems, water heating systems, waste heat recovery and solar power plants etc.

477

478 5. Acknowledgement

479 The authors would like to appreciate and acknowledge Bournemouth University, UK and National
480 University of Sciences and Technology (NUST), Pakistan to support and sponsor for conducting this
481 research.

- 483 [1] M.Z. Jacobson. Review of solutions to global warming, air pollution, and energy security. *Energy*
484 & *Environmental Science*. 2 (2009) 148-73.
- 485 [2] S. Suranovic. Fossil fuel addiction and the implications for climate change policy. *Global*
486 *Environmental Change*. 23 (2013) 598-608.
- 487 [3] International Energy Agency (IEA). *Energy and Climate Change 21st UN Conference of the Parties*
488 (COP21), Paris, 2015.
- 489 [4] J.P. da Cunha, P. Eames. Thermal energy storage for low and medium temperature applications
490 using phase change materials—a review. *Applied Energy*. 177 (2016) 227-38.
- 491 [5] M.M. Farid, A.M. Khudhair, S.A.K. Razack, S. Al-Hallaj. A review on phase change energy storage:
492 materials and applications. *Energy conversion and management*. 45 (2004) 1597-615.
- 493 [6] A. Sharma, V.V. Tyagi, C. Chen, D. Buddhi. Review on thermal energy storage with phase change
494 materials and applications. *Renewable and Sustainable energy reviews*. 13 (2009) 318-45.
- 495 [7] N. Soares, J. Costa, A. Gaspar, P. Santos. Review of passive PCM latent heat thermal energy
496 storage systems towards buildings' energy efficiency. *Energy and buildings*. 59 (2013) 82-103.
- 497 [8] Y. Tian, C.-Y. Zhao. A review of solar collectors and thermal energy storage in solar thermal
498 applications. *Applied Energy*. 104 (2013) 538-53.
- 499 [9] A. Waqas, Z.U. Din. Phase change material (PCM) storage for free cooling of buildings—a review.
500 *Renewable and sustainable energy reviews*. 18 (2013) 607-25.
- 501 [10] L. Miró, J. Gasia, L.F. Cabeza. Thermal energy storage (TES) for industrial waste heat (IWH)
502 recovery: a review. *Applied Energy*. 179 (2016) 284-301.
- 503 [11] A. Modi, F. Bühler, J.G. Andreasen, F. Haglind. A review of solar energy based heat and power
504 generation systems. *Renewable and Sustainable Energy Reviews*. 67 (2017) 1047-64.
- 505 [12] A. Shukla, K. Kant, A. Sharma. Solar Still with latent heat energy storage: A review. *Innovative*
506 *Food Science & Emerging Technologies*. (2017).
- 507 [13] L.F. Cabeza, A. Castell, C.d. Barreneche, A. De Gracia, A. Fernández. Materials used as PCM in
508 thermal energy storage in buildings: a review. *Renewable and Sustainable Energy Reviews*. 15 (2011)
509 1675-95.
- 510 [14] Z. Khan, Z. Khan, A. Ghafoor. A review of performance enhancement of PCM based latent heat
511 storage system within the context of materials, thermal stability and compatibility. *Energy*
512 *Conversion and Management*. 115 (2016) 132-58.
- 513 [15] S. Jegadheeswaran, S.D. Pohekar. Performance enhancement in latent heat thermal storage
514 system: a review. *Renewable and Sustainable Energy Reviews*. 13 (2009) 2225-44.
- 515 [16] L. Fan, J.M. Khodadadi. Thermal conductivity enhancement of phase change materials for
516 thermal energy storage: a review. *Renewable and Sustainable Energy Reviews*. 15 (2011) 24-46.
- 517 [17] P.B. Salunkhe, P.S. Shembekar. A review on effect of phase change material encapsulation on
518 the thermal performance of a system. *Renewable and Sustainable Energy Reviews*. 16 (2012) 5603-
519 16.
- 520 [18] J. Khodadadi, L. Fan, H. Babaei. Thermal conductivity enhancement of nanostructure-based
521 colloidal suspensions utilized as phase change materials for thermal energy storage: a review.
522 *Renewable and Sustainable Energy Reviews*. 24 (2013) 418-44.
- 523 [19] N.S. Dhaidan, J. Khodadadi. Melting and convection of phase change materials in different
524 shape containers: A review. *Renewable and Sustainable Energy Reviews*. 43 (2015) 449-77.
- 525 [20] C. Liu, Z. Rao, J. Zhao, Y. Huo, Y. Li. Review on nanoencapsulated phase change materials:
526 Preparation, characterization and heat transfer enhancement. *Nano Energy*. 13 (2015) 814-26.
- 527 [21] J. Giro-Paloma, M. Martínez, L.F. Cabeza, A.I. Fernández. Types, methods, techniques, and
528 applications for microencapsulated phase change materials (MPCM): a review. *Renewable and*
529 *Sustainable Energy Reviews*. 53 (2016) 1059-75.
- 530 [22] L. Liu, D. Su, Y. Tang, G. Fang. Thermal conductivity enhancement of phase change materials for
531 thermal energy storage: A review. *Renewable and Sustainable Energy Reviews*. 62 (2016) 305-17.

532 [23] F. Agyenim, N. Hewitt, P. Eames, M. Smyth. A review of materials, heat transfer and phase
533 change problem formulation for latent heat thermal energy storage systems (LHTESS). *Renewable*
534 *and sustainable energy reviews*. 14 (2010) 615-28.

535 [24] S. Seddegh, X. Wang, M.M. Joybari, F. Haghghat. Investigation of the effect of geometric and
536 operating parameters on thermal behavior of vertical shell-and-tube latent heat energy storage
537 systems. *Energy*. (2017).

538 [25] M.Y. Yazici, M. Avci, O. Aydin, M. Akgun. On the effect of eccentricity of a horizontal tube-in-
539 shell storage unit on solidification of a PCM. *Applied Thermal Engineering*. 64 (2014) 1-9.

540 [26] S. Seddegh, X. Wang, A.D. Henderson. A comparative study of thermal behaviour of a horizontal
541 and vertical shell-and-tube energy storage using phase change materials. *Applied Thermal*
542 *Engineering*. 93 (2016) 348-58.

543 [27] M. Longeon, A. Soupart, J.-F. Fourmigué, A. Bruch, P. Marty. Experimental and numerical study
544 of annular PCM storage in the presence of natural convection. *Applied energy*. 112 (2013) 175-84.

545 [28] M. Hosseini, M. Rahimi, R. Bahrampoury. Experimental and computational evolution of a shell
546 and tube heat exchanger as a PCM thermal storage system. *International Communications in Heat*
547 *and Mass Transfer*. 50 (2014) 128-36.

548 [29] M. Avci, M.Y. Yazici. Experimental study of thermal energy storage characteristics of a paraffin
549 in a horizontal tube-in-shell storage unit. *Energy conversion and management*. 73 (2013) 271-7.

550 [30] W.-W. Wang, K. Zhang, L.-B. Wang, Y.-L. He. Numerical study of the heat charging and
551 discharging characteristics of a shell-and-tube phase change heat storage unit. *Applied Thermal*
552 *Engineering*. 58 (2013) 542-53.

553 [31] A. Agarwal, R. Sarviya. An experimental investigation of shell and tube latent heat storage for
554 solar dryer using paraffin wax as heat storage material. *Engineering Science and Technology, an*
555 *International Journal*. 19 (2016) 619-31.

556 [32] Z. Meng, P. Zhang. Experimental and numerical investigation of a tube-in-tank latent thermal
557 energy storage unit using composite PCM. *Applied Energy*. 190 (2017) 524-39.

558 [33] Y. Wang, L. Wang, N. Xie, X. Lin, H. Chen. Experimental study on the melting and solidification
559 behavior of erythritol in a vertical shell-and-tube latent heat thermal storage unit. *International*
560 *Journal of Heat and Mass Transfer*. 99 (2016) 770-81.

561 [34] J. Liu, C. Xu, X. Ju, B. Yang, Y. Ren, X. Du. Numerical investigation on the heat transfer
562 enhancement of a latent heat thermal energy storage system with bundled tube structures. *Applied*
563 *Thermal Engineering*. 112 (2017) 820-31.

564 [35] A.A.R. Darzi, M. Jourabian, M. Farhadi. Melting and solidification of PCM enhanced by radial
565 conductive fins and nanoparticles in cylindrical annulus. *Energy Conversion and Management*. 118
566 (2016) 253-63.

567 [36] Z. Li, Z.-G. Wu. Analysis of HTFs, PCMs and fins effects on the thermal performance of shell-tube
568 thermal energy storage units. *Solar Energy*. 122 (2015) 382-95.

569 [37] M.K. Rathod, J. Banerjee. Thermal performance enhancement of shell and tube Latent Heat
570 Storage Unit using longitudinal fins. *Applied thermal engineering*. 75 (2015) 1084-92.

571 [38] C. Liu, D. Groulx. Experimental study of the phase change heat transfer inside a horizontal
572 cylindrical latent heat energy storage system. *International Journal of Thermal Sciences*. 82 (2014)
573 100-10.

574 [39] A.A. Al-Abidi, S. Mat, K. Sopian, M. Sulaiman, A.T. Mohammad. Numerical study of PCM
575 solidification in a triplex tube heat exchanger with internal and external fins. *International journal of*
576 *heat and mass transfer*. 61 (2013) 684-95.

577 [40] S. Almsater, A. Alemu, W. Saman, F. Bruno. Development and experimental validation of a CFD
578 model for PCM in a vertical triplex tube heat exchanger. *Applied Thermal Engineering*. 116 (2017)
579 344-54.

580 [41] M. Kabbara, D. Groulx, A. Joseph. Experimental investigations of a latent heat energy storage
581 unit using finned tubes. *Applied Thermal Engineering*. 101 (2016) 601-11.

582 [42] F. Agyenim, P. Eames, M. Smyth. A comparison of heat transfer enhancement in a medium
583 temperature thermal energy storage heat exchanger using fins. *Solar Energy*. 83 (2009) 1509-20.
584 [43] S. Lohrasbi, M. Gorji-Bandpy, D.D. Ganji. Thermal penetration depth enhancement in latent heat
585 thermal energy storage system in the presence of heat pipe based on both charging and discharging
586 processes. *Energy Conversion and Management*. 148 (2017) 646-67.
587 [44] A. Caron-Soupart, J.-F. Fourmigué, P. Marty, R. Couturier. Performance analysis of thermal
588 energy storage systems using phase change material. *Applied Thermal Engineering*. 98 (2016) 1286-
589 96.
590 [45] Z. Khan, Z. Khan, K. Tabeshf. Parametric investigations to enhance thermal performance of
591 paraffin through a novel geometrical configuration of shell and tube latent thermal storage system.
592 *Energy Conversion and Management*. 127 (2016) 355-65.
593 [46] Z. Khan, Z.A. Khan. Experimental investigations of charging/melting cycles of paraffin in a novel
594 shell and tube with longitudinal fins based heat storage design solution for domestic and industrial
595 applications. *Applied Energy*. (2017).
596 [47] Rubitherm® Technologies GmbH, <http://www.rubitherm.eu/en/>. 2017.

597